J. Korean Inst. Electr. Electron. Mater. Eng.
Vol. 37, No. 2, pp. 188-194 March 2024
DOI: https://doi.org/10.4313/JKEM.2024.37.2.10
ISSN 1226-7945(Print), 2288-3258(Online)

Regular Paper

Optimized O_2 Plasma Surface Treatment for Uniform Sphere Lithography on Hydrophobic Photoresist Surfaces

Yebin Ahn, Jongchul Lee, Hanseok Kwon, Jungbin Hong, and Han-Don Um

Department of Chemical Engineering, Kangwon National University, Chuncheon 24341, Korea

(Received December 17, 2023; Revised December 28, 2023; Accepted January 2, 2024)

Abstract: This paper introduces an optimized oxygen (O_2) plasma surface treatment technique to enhance sphere lithography on hydrophobic photoresist surfaces. The focus is on semiconductor manufacturing, particularly the creation of finer structures beyond the capabilities of traditional photolithography. The key breakthrough is a method that makes substrate surfaces hydrophilic without altering photoresist patterns. This is achieved by meticulously controlling the O_2 plasma treatment duration. The result is the consistent formation of nano and microscale patterns across large areas. From an academic perspective, the study deepens our understanding of surface treatments in pattern formation. Industrially, it heralds significant progress in semiconductor and precision manufacturing sectors, promising enhanced capabilities and efficiency.

Keywords: Lithography, Photolithography, Sphere lithography, Polystyrene sphere, O_2 plasma, Contact angle

1. INTRODUCTION

The modern semiconductor industry continuously evolves towards higher integration and miniaturization [1-4]. For the integration circuit process, photolithography is a key process in forming semiconductor circuit patterns. The photolithography process utilizes light to create fine structures on semiconductor wafers. Recent advancements in semiconductor technology demand even finer structures, prompting research into next-generation technologies such as gate-all-around structures. These technologies require the formation of structures on the scale of a few nanometers, necessitating overcoming limitations in existing photolithography techniques. To fabricate nanopatterns by photolithography, extreme ultraviolet (EUV) lithography with a short wavelength of 13.5 nm is gaining attention [5,6]. However, such techniques require highly expensive equipment, limiting accessibility for universities and research institutions.

As an alternative to form the nanopattern, sphere lithography has emerged. This technique involves using nano-sized spheres, such as SiO_2 [7,8] or polystyrene [9-12], to form a monolayer on a substrate, creating nanometer-sized structures. Sphere lithography has attracted significant attention due to its simple and cost-effective method [13-15]. The inter-sphere attraction force in nano-spheres enables the formation of a densely packed monolayer. Consequently, by forming a close-packed array, the spacing between spheres can be adjusted according to the diameter of the nano-spheres. However, sphere lithography is limited to spacings determined by the diameter of the nano-spheres and can only form patterns within the hexagonal arrangement of a close-packed array. Therefore, it has limitations in implementing the diverse patterns and spacings required for semiconductor devices such as transistors, diodes, and sensors.

To overcome these limitations, this paper proposes a hybrid lithography technique that combines the advantages of photolithography and sphere lithography. This technique is

✉ **Han-Don Um; handon@kangwon.ac.kr**

capable of simultaneously forming structures at both nano and micro scales, particularly by applying sphere lithography on micropattern defined by photolithography. This approach allows for the effective formation of complex patterns and structures of various sizes. For the uniform pattern by the sphere lithography, the hydrophilic surfaces play an essential role in the arrangement and uniformity of the spheres. However, the photoresist used in photolithography tends to make surfaces hydrophobic, posing challenges in harmonizing the two techniques. To address this issue, we applied an O_2 plasma surface treatment process to hydrophilize surfaces treated with photoresist.

O_2 plasma surface treatment enhances surface hydrophilicity, improving the uniformity of sphere lithography but can etch preformed photoresist structures on the substrate, leading to challenges in process control. First, we investigated the morphological characteristics of the photoresist according to the exposed energy of the photolithography. Then, we optimized the O_2 plasma process time to enhance surface hydrophilicity while minimizing the over-etch of photoresist. Surface contact angle measurements were used to quantitatively assess hydrophilicity, and the deformation of the photoresist under various O_2 plasma treatment conditions was also observed. This experimental approach provided a critical solution for maximizing the uniformity of sphere lithography while maintaining the precision of photolithography. These results are expected to open up possibilities for applications not only in semiconductor processes but also in other high-precision manufacturing fields like micro-electro-mechanical systems (MEMS). Especially in fields requiring complex structures at nano and micro scales, this hybrid lithography technique could offer a new manufacturing methodology for enhancing the efficiency and precision of semiconductor manufacturing processes.

2. EXPERIMENTS

Photolithography process: The p-type (100) Si wafers with a resistivity range of 1~10 ohm.cm was used. To form the hydrophobic surface of the Si wafer, hexamethyldisilazane (HMDS, 96%, Daejung Chemical) was spin-coated onto the wafer at 1,500 rpm for 40 sec. Subsequently, the negative photoresist (DNR-L300-D1, Dongjin Semi Cam) was spin-coated at 4,000 rpm, followed by a soft bake at 100°C for 60 sec to remove residual solvents. The coated wafer was exposed to ultraviolet (UV) light by a photoaligner (Prowin, M100) with an energy range of 200 to 500 mJ/cm^2 to define the desired patterns. After exposure to UV light, a post-exposure bake was conducted at 110°C for 90 sec. The photoresist patterns were developed by immersing the Si wafer in a tetramethylammonium hydroxide (TMAH) solution (25% solution in water, Merck) for approximately 2 min. This step led to the creation of the intended structures on the Si wafer surface. The process flow of photolithography is illustrated in Fig. 1(a). The structural analysis of the fabricated patterns was conducted through scanning electron microscopy (SEM, Hitachi S-4800) analysis.

O_2 plasma treatment process: The hydrophilic surface treatment was conducted by using the O_2 plasma system (Femto Science, CIONE4). Base and process pressures were 2.5×10^{-3} Torr and 5×10^{-1} Torr, respectively. The O_2 gas of 30 standard cubic centimeters per minute (sccm) was supplied during the O_2 plasma treatment process. The radio frequency (RF) bias power was 100 watts at 13.5 MHz. The treatment time was controlled from 0 to 25 min. After plasma treatment, the chamber was vented using N_2 gas. Following the treatment process, contact angle measurements were conducted utilizing a contact angle goniometer (Kruss, DE/DSA25) to quantify alterations in surface wettability resulting from the treatment.

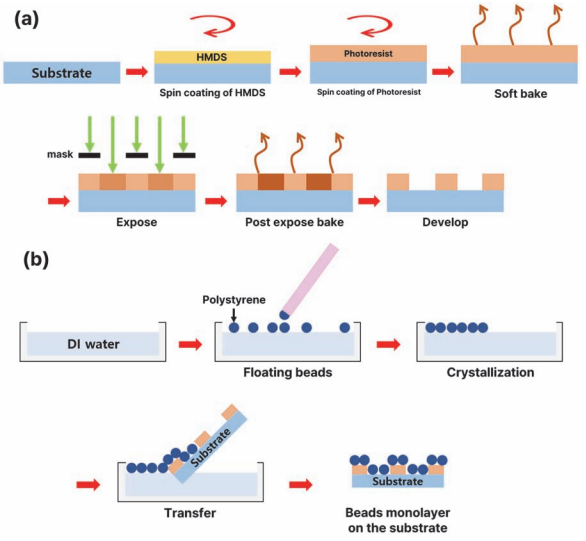

Fig. 1. The process flows of (a) photolithography on bare Si substrate and (b) sphere lithography on pre-patterned substrate.

Sphere lithography: For the sphere lithography process, the polystyrene (PS) sphere solution (2 μm diameter, 1% concentration, Thermo Fisher) was applied. The PS spheres were floated on deionized water using the Langmuir-Blodgett method to achieve a monolayer of floating beads. Subsequently, the PS beads were transferred onto the Si wafer to form a hexagonal arrangement of spheres. To transfer the lithography pattern to the wafer, a thermal evaporator (Woosung Hi-Vac) was used to deposit Aluminum with a thickness of 50 nm onto the lithography pattern. The wafer was then immersed in acetone for 10 min. This process facilitated the lift-off of the photoresist layer and PS spheres, leaving the desired pattern on the Si wafer. The process flow of sphere lithography is illustrated in Fig. 1(b). The morphology and features of the resulting structures were analyzed and characterized using SEM (Hitachi S-4800) and optical microscopy techniques (Radical, RXM-7).

3. RESULTS AND DISCUSSION

In photolithography, the morphological characteristics of photoresists under varying exposure conditions are crucial. Since the photoresist is the negative resist, the areas exposed to light remain as the resist material while removing the unexposed area by the developer. When the negative resist is subjected to critical exposure energy, the resist undergoes a polymer cross-linking reaction. This reaction increases the molecular weight of the resist, making it insoluble in the developer solution, thereby forming a solid structure.

We controlled the exposure energy ranging from 200 to 500 mJ/cm^2. The variations in the structure of the negative depending on the exposure energy can be observed in the SEM images of Figs. 2(a)~(d). We measured the top and bottom diameters, height, and angle of the discs in relation to the substrate as shown in Fig. 2(e). As the exposure energy increases, a trend is observed where both the top and bottom diameters of the photoresist discs increase. This phenomenon can be attributed to the scattering of light within the resist during the exposure as the light, transmitted through the photomask, spreads beyond the size of the holes defined in the photomask. This light scattering causes the actual exposed area on the resist to be larger than the photomask's pattern. These results are observed by comparing Figs. 2(a) and (d). The lowest energy (200 mJ/cm^2) results in a cylindrical structure of the photoresist, whereas the highest energy (500 mJ/cm^2) leads to a tapered structure. This variation in structure is more pronounced as the difference between the top and bottom diameters gradually increases, a trend observable in the graph presented in Fig. 2(e). Consequently, it is noted that the angle of the photoresist structure decreases from 85±5 to 76±13°. The tapering observed at higher energy levels is due to the light scattering over a longer distance as the scattered light penetrates deeper into the photoresist material [16]. This scattering effect elongates the path of the light along the depth of the resist, leading to a broader area of exposure at the bottom compared to the top, hence the tapered shape. While the top and bottom diameters of the photoresist show variations depending on the exposure energy, an interesting observation is that the height of the photoresist remains unchanged. This consistency in height, as depicted in Fig. 2(f),

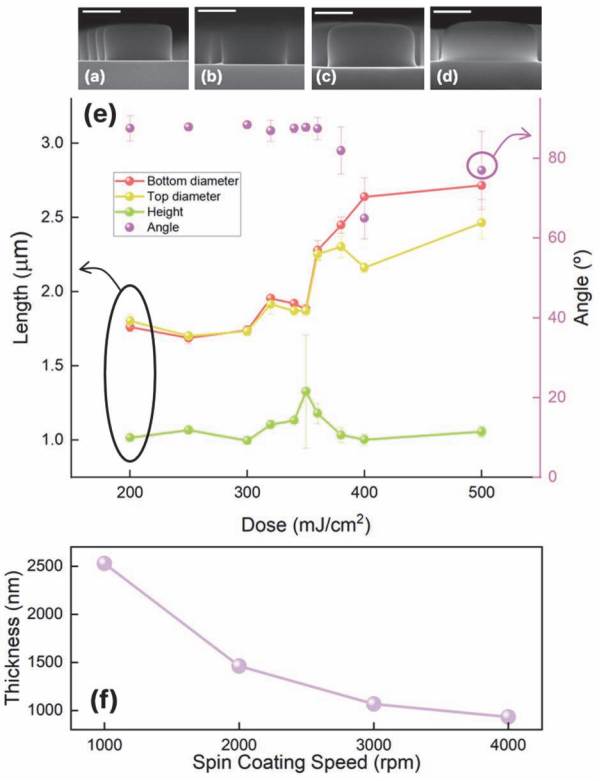

Fig. 2. SEM images in the shape of photoresist as a function of the exposed dose: (a) 200 mJ/cm^2, (b) 300 mJ/cm^2, (c) 360 mJ/cm^2, (d) 500 mJ/cm^2 (the scale bar is 1 μm), (e) bottom diameter, top diameter, height, and angle of photoresist as a function of the exposed dose, and (f) thickness of photoresist as a function of the spin coating speed.

is primarily determined by the spin speed during the spin-coating process. To adjust the height of the photoresist, it is therefore necessary to design and calibrate the coating process accordingly. In other words, while the exposure energy significantly influences the diameter and shape of the photoresist structures, the height is governed by the conditions set during the coating stage. Based on the results of Fig. 2, we found that even with a mask of a fixed diameter, it is possible to control the size and structure of the photoresist by adjusting the exposure energy. This is significant as it offers a method to fine-tune the photolithography process beyond the physical limitations of the photomask. By manipulating the exposure energy, a range of photoresist structures, from cylindrical to tapered, can be achieved.

Sphere lithography has emerged as a cost-effective and scalable method for creating nanostructure arrays. This technique allows for the transfer of simple hexagonal arrays of spheres onto various substrates like polymers [17], glass [18], and semiconductors [19]. The Langmuir-Blodgett method is an innovative approach for fabricating monolayers of two-dimensional colloidal spheres [20-22]. This technique operates by forming the monolayer at the liquid-air interface, which is then strategically transferred onto a solid substrate. The advantage of this method lies in its ability to transfer the monolayer suspended in the solution onto substrates with pre-existing structural patterns. However, the reproducibility of this transfer process heavily depends on the hydrophilic nature of the substrate's surface. To effectively transfer two-dimensional colloidal sphere arrays onto a substrate, it's crucial to modify the surface to become more hydrophilic. The O_2 plasma surface treatment plays a pivotal role in this surface modification process [23]. By enhancing the hydrophilicity of the substrate, this treatment ensures that the colloidal sphere arrays adhere properly and maintain their precision and order during the transfer.

The O_2 plasma treatment process is not only capable of hydrophilizing the surface of a substrate but can also etch polymers, depending on the plasma process conditions. In this study, since the pre-patterned structures were formed by the photoresist, we observed the structural changes in the photoresist with the different etching times of O_2 plasma treatment as shown in the SEM images of Figs. 3(a)~(d). Figure 3(e) shows the rate of change in the top diameter, bottom diameter, and height of the photoresist concerning different etching times. It was observed that the height of the photoresist decreases linearly as the etching time increases. This linear reduction is attributed to the etching of the photoresist by the plasma. Interestingly, while the height shows a consistent decrease, the rates of change in both the top and bottom diameters of the photoresist remain unchanged up to 20 min of etching. However, after 25 min, decreases in the top and bottom diameters are observed. This phenomenon can be explained by the directional nature of the O_2 radicals generated in the plasma [24]. These radicals, accelerated by the bias, tend to etch more vertically than horizontally. As a result, vertical etching is more pronounced compared to horizontal etching in the initial stages. As the etching time is extended, the reaction temperature increases spontaneously, leading to more isotropic etching due to the chemical reactions. This result thus reveals the intricate balance between the etching time and the resulting changes in the photoresist's structure, highlighting the importance of carefully controlling the O_2 plasma treatment time. Based on the results of Fig. 3, the etching time of 20min was determined to achieve the hydrophilic surface while maintaining the original diameters of the photoresist.

To quantitatively assess the hydrophilicity of surfaces, the contact angle was measured. Figure 4(a) presents the results of contact angles measured before and after O_2 plasma treatment.

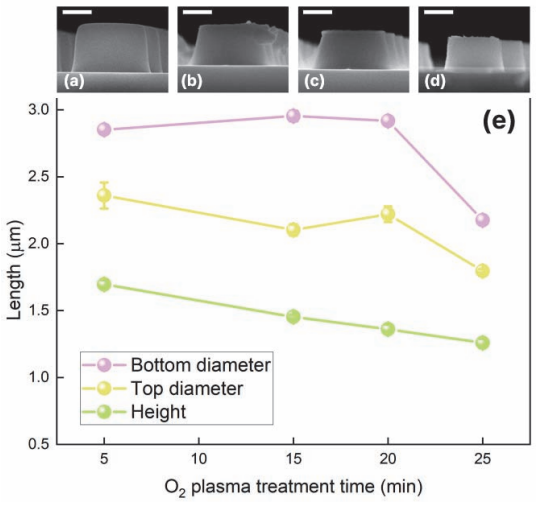

Fig. 3. SEM images in the shape of photoresist as a function of the O_2 plasma process time: (a) 5 min, (b) 15 min, (c) 20 min, (d) 25 min (the scale bar is 1 μm), and (e) top diameter, bottom diameter, and height, of photoresist as a function of the O_2 plasma treatment time.

To figure out the effect of the photoresist pattern, the contact angles of substrates with photoresist patterns were compared to the bare substrate without the photoresist. Before the O_2 plasma treatment, the contact angle on a bare Si substrate without a pattern was measured at 65.1±6°. However, the formation of a photoresist (PR) pattern on the substrate significantly increased the contact angle to 105.0±7°, which indicates an even stronger hydrophobic tendency. After O_2 plasma treatments, significant changes in contact angles were observed. The contact angle on the Si substrate without the photoresist pattern decreased to such an extent that it could not be measured, indicating an extremely high level of wetting. For substrates with the photoresist pattern, the contact angle significantly decreased to 6.1±1°, suggesting a significant increase in hydrophilicity. As shown in the optical photographs in Figs. 4(b) and (c), substrates treated with O_2 plasma exhibit uniform monolayer formation across a large area without defects. This uniformity is further highlighted in the SEM images of the selected areas in Figs. 4(d) and (e). The substrate not treated with O_2 plasma, as seen in Fig. 4(d), displays smaller grain sizes in the monolayer and noticeable gaps between the grains where spheres are absent. In contrast, the substrate treated with O_2 plasma, as illustrated in Fig. 4(e), shows a highly uniform monolayer, with the spheres consistently distributed even over the photoresist.

This surface treatment resulted in the effective formation of hybrid patterns at both the nano and micro scales across a wide area. To transfer these patterns onto the substrate, a 30 nm-thick Al film was deposited over the hybrid pattern. The deposited samples were processed by a lift-off process with acetone as shown in Fig. 5(a). Microholes with diameters of 20 μm, formed from the photoresist, are interspersed with an Al mesh featuring 680 nm linewidths as shown in the SEM images of Figs. 5(b)~(d). This successful implementation of structures at both nanometer and micrometer dimensions on a single substrate demonstrates the versatility of using photoresist, allowing for a wide range of patterns without limitations on size or shape. Between the micropatterns, a fine mesh with narrow line widths can be created. Such high structural freedom is anticipated to be highly beneficial in various applications in MEMS and nanoelectromechanical systems (NEMS), offering diverse utility due to the capability to fabricate intricate and precise patterns.

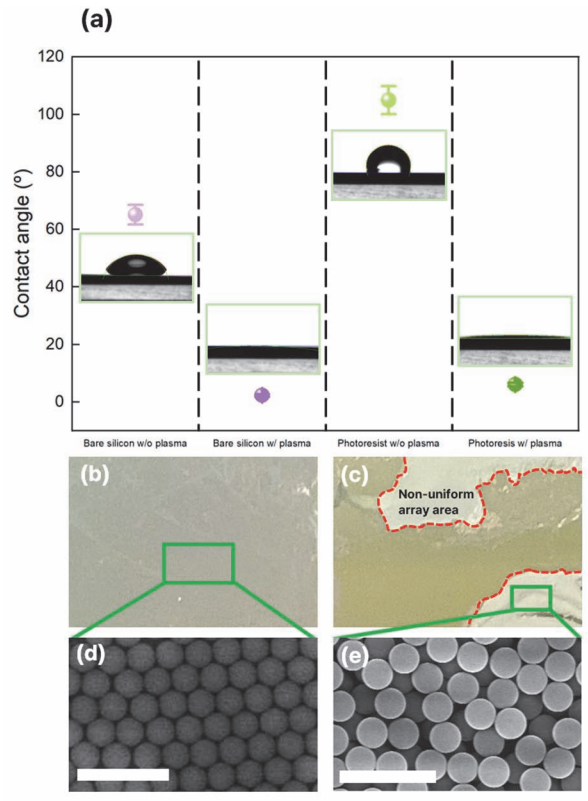

Fig. 4. (a) Contact angles of various substrates as a function of the O_2 plasma process. Optical images of the photoresist substrates (b) with and (c) without O_2 plasma treatment. (d), (e) SEM images of the regions marked by the green boxes in panels (b) and (c), respectively. The scale bar is 6 μm.

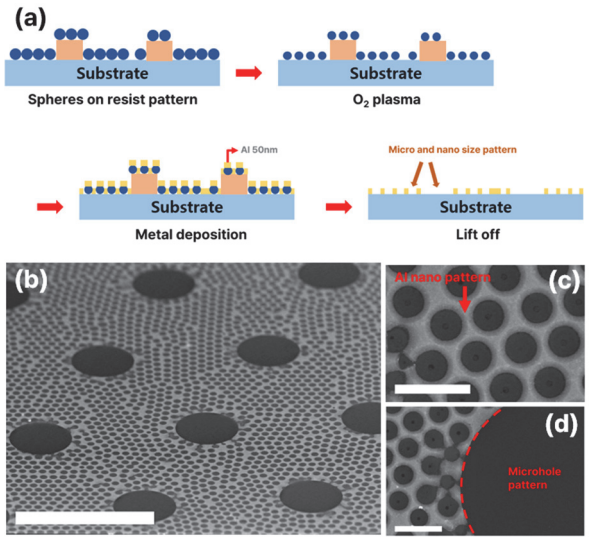

Fig. 5. (a) Process flow of lift-off combined with hybrid lithography, (b) low and (c), (d) high magnification SEM images after the lift-off process [the scale bars of panel (b), (c), and (d) are 40 μm, 5 μm, and 5 μm, respectively].

4. CONCLUSIONS

The research successfully demonstrates an optimized O_2 plasma surface treatment as a crucial factor in developing uniform nano and microscale hybrid patterns on hydrophobic photoresist surfaces. Through precise control of the O_2 plasma treatment time, the study achieves hydrophilization of the substrate without altering the photoresist patterns, ensuring the integrity of the original designs. The effective transfer of these intricate patterns onto substrates signifies a significant advancement in sphere lithography and holds promising implications for semiconductor manufacturing and precision engineering fields. The study concludes that this innovative approach facilitates the creation of complex, large-area patterns with high uniformity, opening new avenues in MEMS and NEMS applications.

ORCID

Han-Don Um https://orcid.org/0000-0002-2087-160X

ACKNOWLEDGMENTS

This study was supported by 2021 Research Grant from Kangwon National University. This work was also supported by the National Research Foundation of Korea (NRF) grant funded by the Korea government (MSIT) (No.2022R1C1C 1010025). Following are the results of a study on the 'Leaders in INdustry-university Cooperation 3.0' Project, supported by the Ministry of Education and National Research Foundation of Korea.

REFERENCES

[1] S. Wei, Z. Li, A. John, B. I. Karawdeniya, Z. Li, F. Zhang, K. Vora, H. H. Tan, C. Jagadish, K. Murugappan, A. Tricoli, and L. Fu, *Adv. Funct. Mater.*, **32**, 2107596 (2022). doi: https://doi.org/10.1002/ADFM.202107596

[2] E. Mullen and M. A. Morris, *Nanomaterials*, **11**, 1085 (2021). doi: https://doi.org/10.3390/NANO11051085

[3] A. V. Vorotyntsev, A. N. Petukhov, M. M. Trubyanov, A. A. Atlaskin, D. A. Makarov, M. S. Sergeeva, I. V. Vorotyntsev, and V. M. Vorotyntsev, *Rev. Chem. Eng.*, **37**, 125 (2021). doi: https://doi.org/10.1515/REVCE-2018-0046

[4] N. Shin, K. L. Kraemer, and J. Dedrick, *Ind. Innovation*, **24**, 280 (2017). doi: https://doi.org/10.1080/13662716.2016.1224708

[5] T. Manouras and P. Argitis, *Nanomaterials*, **10**, 1593 (2020). doi: https://doi.org/10.3390/NANO10081593

[6] T. Kozawa, *Jpn. J. Appl. Phys.*, **58**, 096502 (2019). doi: https://doi.org/10.7567/1347-4065/AB37FF

[7] Y.F.C. Chau, C. J. Lin, T. S. Kao, Y. C. Wang, C. M. Lim, N.T.R.N. Kumara, and H. P. Chiang, *Results Phys.*, **17**, 103168 (2020). doi: https://doi.org/10.1016/J.RINP.2020.103168

[8] L. N. Dvoretckaia, A. M. Mozharov, and I. S. Mukhin, *J. Phys.: Conf. Ser.*, **917**, 062062 (2017). doi: https://doi.org/10.1088/1742-6596/917/6/062062

[9] E. A. Vyacheslavova, I. A. Morozov, D. A. Kudryashov, and A. S. Gudovskikh, *J. Phys.: Conf. Ser.*, **1697**, 012188 (2020). doi: https://doi.org/10.1088/1742-6596/1697/1/012188

[10] A. Chandramohan, N. V. Sibirev, V. G. Dubrovskii, M. C. Petty, A. J. Gallant, and D. A. Zeze, *Sci. Rep.*, **7**, 40888 (2017). doi: https://doi.org/10.1038/srep40888

[11] E. Cara, F. F. Lupi, M. Fretto, N. De Leo, M. Tortello, R. Gonnelli, K. Sparnacci, and L. Boarino, *Nanomaterials*, **10**, 280 (2020). doi: https://doi.org/10.3390/NANO10020280

[12] L. Luo, E. M. Akinoglu, L. Wu, T. Dodge, X. Wang, G. Zhou, M. J. Naughton, K. Kempa, and M. Giersig, *Nanotechnology*, **31**, 245302 (2020). doi: https://doi.org/10.1088/1361-6528/AB7C4C

[13] M. Pisco, F. Galeotti, G. Quero, G. Grisci, A. Micco, L. V. Mercaldo, P. D. Veneri, A. Cutolo, and A. Cusano, *Light: Sci. Appl.*, **6**, e16229 (2017). doi: https://doi.org/10.1038/lsa.2016.229

[14] L. N. Dvoretckaia, A. M. Mozharov, Y. Berdnikov, and I. S. Mukhin, *J. Phys. D: Appl. Phys.*, **55**, 09LT01 (2021). doi: https://doi.org/10.1088/1361-6463/AC368D

[15] J. Y. Choi and C. B. Honsberg, *Appl. Sci.*, **8**, 1720 (2018). doi: https://doi.org/10.3390/APP8101720

[16] P. Dentinger, G. Cardinale, C. Henderson, A. Fisher, and A. Ray-Chaudhuri, *Photoresist Film Thickness for Extreme Ultraviolet Lithography*, (2000). doi: https://doi.org/10.1117/12.390098

[17] O. Brüggemann, K. Haupt, L. Ye, E. Yilmaz, and K. Mosbach, *J. Chromatogr. A*, **889**, 15 (2000). doi: https://doi.org/10.1016/S0021-9673(00)00350-2

[18] Z. Zhong, Y. Yin, B. Gates, and Y. Xia, *Adv. Mater.*, **12**, 206 (2000). doi: https://doi.org/10.1002/(SICI)1521-4095(200002)12:3<206::AID-ADMA206>3.0.CO;2-5

[19] F. J. Wendisch, M. Abazari, H. Mahdavi, M. Rey, N. Vogel, M. Musso, O. Diwald, and G. R. Bourret, *ACS Appl. Mater. Interfaces*, **12**, 13140 (2020). doi: https://doi.org/10.1021/ACSAMI.9B21466

[20] F. J. Wendisch, M. Rey, N. Vogel, and G. R. Bourret, *Chem. Mater.*, **32**, 9425 (2020).
doi: https://doi.org/10.1021/ACS.CHEMMATER.0C03593

[21] M. Rey, M. A. Fernandez-Rodriguez, M. Karg, L. Isa, and N. Vogel, *Acc. Chem. Res.*, **53**, 414 (2020).
doi: https://doi.org/10.1021/ACS.ACCOUNTS.9B00528

[22] J.S.J. Tang, R. S. Bader, E.S.A. Goerlitzer, J. F. Wendisch, G. R. Bourret, M. Rey, and N. Vogel, *ACS Omega*, **3**, 12089 (2018).
https://doi.org/10.1021/ACSOMEGA.8B01985

[23] C. Satriano, G. Marietta, and B. Kasemo, *Surf. Interface Anal.*, **40**, 649 (2008).
doi: https://doi.org/10.1002/SIA.2764

[24] X. Zhang, L. Lei, B. Xia, Y. Zhang, and J. Fu, *Electrochim. Acta*, **54**, 2810 (2009).
doi: https://doi.org/10.1016/J.ELECTACTA.2008.11.029